CRYSTAL GROWTH & DESIGN

Article

pubs.acs.org/crystal

Temperature, Cooling Rate, and Additive-Controlled Supramolecular Isomerism in Four Pb(II) Coordination Polymers with an in Situ Ligand Transformation Reaction

Dongsheng Deng,[†] Leilei Liu,[§] Bao-Ming Ji,*[,†] Guojie Yin,[†,‡] and Chenxia Du*[,‡]

[†]College of Chemistry and Chemical Engineering, Luoyang Normal University, Luoyang 471022, People's Republic of China

[‡]Department of Chemistry, Zhengzhou University, Zhengzhou 450052, People's Republic of China

[§]College of Chemistry and Chemical Engineering, Anyang Normal University, Anyang 455000, People's Republic of China

Supporting Information

ABSTRACT: Solvothermal reactions of $Pb(Ac)_2$ with a new flexible 1,3-bis(4-pyridyl-3-cyano)propane (**1**, BPCP) ligand under different synthesis conditions via an in situ ligand transformation reaction produced three true coordination polymorphs, namely, $[PbL^{2-}]_n$ (for **2** and **3**) and $[Pb_3L^{2-}{}_3]_n$ (**4**), as well as their polymorphic framework $[(Pb_2L^{2-})\cdot 2H_2O]_n$ (**5**) (H_2L = 1,3-bis(4-pyridyl-3-carboxyl)-propane). These compounds were characterized by elemental analysis, IR, TG, PXRD, and single-crystal X-ray diffraction. In these compounds, the L^{2-}ligand exhibits different coordination conformations and modes tuned by different synthesis conditions, including reaction temperature, cooling rate, and additive, and constructs various architectures by bridging a variety of building units. Polymorphs **2** and **3** display a 3D framework with 1D channels built up from dinuclear ringlike $[Pb_2L^{2-}{}_2]$ units and dinuclear semi-ring-like $[Pb_2L^{2-}]$ units, respectively. Polymorph **4** also features a 3D architecture constructed from dinuclear ringlike $[Pb_2L^{2-}{}_2]$ units interlinked by the L^{2-} ligand. Interestingly, the framework of **4** is big enough to allow the other net to penetrate to form a 2-fold interpenetrating framework with a trinodal (3,6,10)-connected topology with a point symbol of $(4^3)(4^4\cdot 6^{10}\cdot 8)(4^8\cdot 6^{24}\cdot 8^9\cdot 10^4)$. For **5**, there exists two kinds of dinuclear ringlike $[Pb_2L^{2-}{}_2]$ units. These $[Pb_2L^{2-}{}_2]$ units are interconnected by Pb atoms to afford a 2D undulant network that is further connected by the hydrogen-bonding interactions and weak interactions to afford a 3D supramolecular network. In addition, the photoluminescence properties of **1**−**5** and the H_2L ligand in the solid state at room temperature were also investigated.

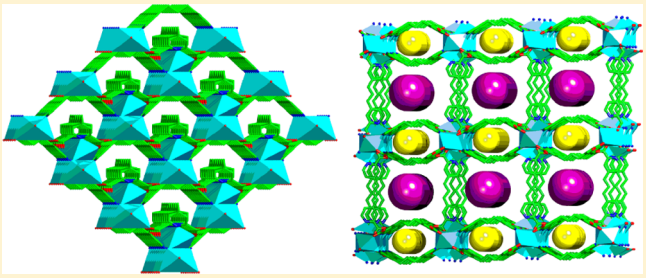

INTRODUCTION

Supramolecular isomerism, as coined by Zaworotko, is used to describe the existence of more than one type of network superstructure for a given set of components.[1] In some instances, supramolecular isomerism can be synonymous with polymorphism that is an intriguing phenomenon in crystal engineering. However, in other situations, supramolecular isomers are not true polymorphs for their different chemical compositions caused by the coexistence of different guest molecules.[1d] In this context, the term *polymorphic frameworks* was defined by Matzger to better describe these different architectures or superstructures with the existence of guest or solvent molecules.[2] Because of the dissimilarity in crystal structures, supramolecular isomers (including polymorphs and polymorphic frameworks) can vary significantly in their physicochemical properties. An understanding of the relationship between the structure and property in supramolecular isomers is particularly important as epitomized by the fast growing number of crystal structures in the Cambridge Structural Database (CSD)[3] as well as the rapidly expanding scope of attention and a great many research reports on supramolecular isomers.[4] However, methods of controlling the synthetic pathways are required for the rational design of supramolecular isomers with unique structures and properties, and it is generally difficult to structurally predict for complexes produced by new components.[5] In comparison to supramolecular isomers with different chemical compositions due to the coexistence of guest components,[1c,6] polymorphs with a fixed stoichiometry for all components are particularly rare for coordination polymers (CPs),[7] although it is widely observed for organic compounds.[8]

Currently, the self-assembly of coordination polymers depends on many factors, such as the nature of the metal ion,[9] structural features of the organic ligand,[10] counterion,[11] and a number of experimental variables containing reaction temperature, reagent ratio, pH value, solvent system, and the methods of the crystallization.[12] Most research results suggest that a subtle alteration by means of these factors can lead to totally different products.[13] In this regard, reaction temperature has been verified as a crucial parameter in influencing the

Received: July 12, 2012
Revised: September 28, 2012
Published: October 10, 2012

   dx.doi.org/10.1021/cg300900m | *Cryst. Growth Des.* 2012, 12, 5338−5348

Scheme 1. Synthetic Route of H_2L Ligand

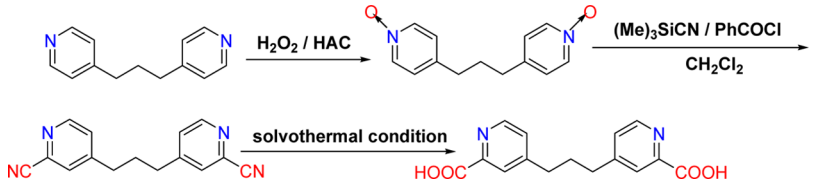

Scheme 2. Possible Conformations of H_2L Ligand

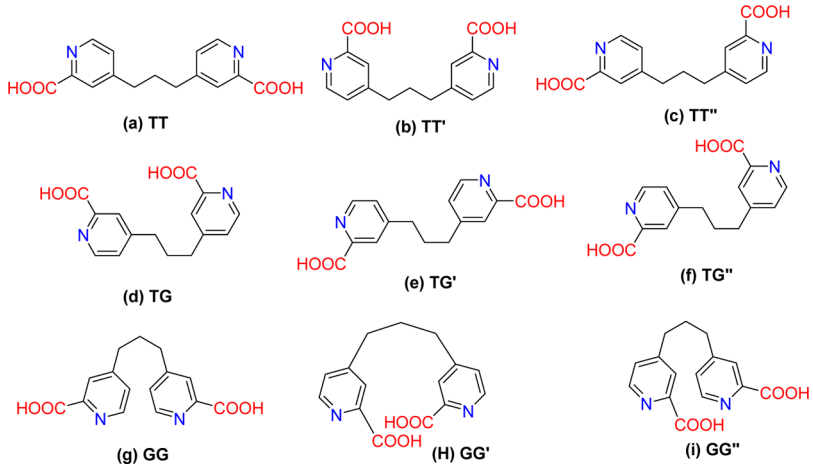

formation of CPs with variable topologies based upon the conformations of ligands.[14] It is well-known that flexible organic linkers inherently hold the potential of adopting different conformations under different conditions, especially at different temperatures.[15] The thermodynamically favored conformer associated with a large activation barrier can be achieved at high temperature, whereas low temperature favors the kinetic conformer because the thermal energy relies on the temperature proportionally. Therefore, the thermodynamically or kinetically favored conformers could be obtained by carefully controlling the reaction temperature.[14,16] Accordingly, it is expected that the reaction temperature should play an additional crucial factor in determining the CP topology and the dimensionality of the structures through controlling the ligand conformation.

On the other hand, most of the research on CPs so far has focused on d-block transition CPs, and p-block main CPs have been relatively less explored. Compared with the transition-metal atoms, the main group metal lead atom, with a larger radius and $[Xe]4f^{12}5d^{10}6s^26p^2$ electronic configurations, can give the Pb(II) cation variable coordination numbers (from 2 to 10), which provide unique opportunities for the construction of novel network topologies and some fascinating physical properties.[17] Thus, lead-based structural chemistry has recently been receiving increasing attention due to its fantastic architectures and good physical properties.

In the light of the above-mentioned motivations, we are focusing our attention on using a novel 1,3-di(4-pyridyl-3-cyano)propane ligand (BPCP, Scheme 1), as the flexible ligand to construct CPs, which is based mostly on the following considerations: (1) Two cyano groups of BPCP could be easily hydrolyzed to carboxylic groups through an in situ ligand transformation reaction under solvothermal conditions, and the resulting flexible dicarboxylate linker (H_2L = 1,3-di(4-pyridyl-3-carboxyl)propane) shows a much greater thermal stability. Therefore, this lignand has the ability to provide insight into supramolecular isomerism or polymorphism, similar to that observed in the previous reports.[6] (2) The H_2L ligand has a relatively longer spacer, and the two pyridyl groups can rotate along its C−C bonds to form six configurations (Scheme 2). Thereby, we anticipated that the conformational changes of the H_2L ligand could be controlled by regulating solvothermal reaction conditions, which maybe lead to the generation of various coordination polymers with different topological structures. Fortunately, the foregoing effort has led to the isolation of three true polymorphs, $[PbL^{2-}]_n$ (for **2** and **3**), $[Pb_3L^{2-}{}_3]_n$ (**4**), and their polymorphic frameworks $[(Pb_2L^{2-}{}_2)\cdot 2H_2O]_n$ (**5**), with entirely distinct topological networks by the assembly of Pb(II) acetate with the H_2phda ligand under different solvothermal reaction conditions, including different temperatures, reaction components, and crystallization conditions. Herein, we will present the in situ syntheses, crystal structures, and thermal and photoluminescenct properties of compounds **1**−**5**.

EXPERIMENTAL SECTION

General Procedure. 1,3-Bis(4-pyridyl)propane-*N*,*N*′-dioxide was prepared according to the literature methods.[18] All chemicals and reagents were obtained from commercial sources and used as received. The IR spectra were recorded on a Nicolet 6700 FT-IR spectrometer in the 4000−400 cm^{-1} region. Elemental analyses for C, H, and N were carried out on a Flash 2000 elemental analyzer. Powder X-ray diffraction (PXRD) measurements were performed on a Bruker D8-ADVANCE X-ray diffractometer with Cu Kα (λ = 1.5418 Å). Luminescent spectra were recorded with a Rigaku RIX 2000 fluorescence spectrophotometer. Thermogravimetric analyses were carried out on a SDT Q600 thermogravimetric analyzer. A platinum pan was used for heating the sample with a heating rate of 10 °C/min under a N_2 atmosphere.

Preparation of 1,3-bis(4-pyridyl-3-cyano)propane (BPCP, 1). To a solution of 1,3-bis(4-pyridyl)propane-*N*,*N*′-dioxide (4.61 g, 20 mmol) in CH_2Cl_2 (280 mL) was added 26.67 mL of Me_3SiCN (200 mmol) with stirring at 0 °C. After stirring for 2 h, 9.28 mL of benzoyl

dx.doi.org/10.1021/cg300900m | Cryst. Growth Des. 2012, 12, 5338−5348

Table 1. Summary of Crystallographic Data for 1−5

	1	2	3	4	5
empirical formula	$C_{15}H_{12}N_4$	$C_{15}H_{12}N_2O_4Pb$	$C_{15}H_{12}N_2O_4Pb$	$C_{45}H_{36}N_6O_{12}Pb_3$	$C_{30}H_{28}N_4O_{10}Pb_2$
fw	248.29	491.47	491.46	1474.40	1018.96
cryst syst	triclinic	monoclinic	orthorhombic	monoclinic	triclinic
space group	$P\bar{1}$	$P2_1/c$	$Fdd2$	$C2/m$	$P\bar{1}$
a (Å)	6.8839(15)	12.5956(17)	14.2347(12)	22.976(13)	11.795(2)
b (Å)	8.8678(19)	13.2999(18)	19.772(2)	19.587(11)	13.2729(11)
c (Å)	10.965(2)	9.7711(13)	10.8817(10)	10.776(6)	13.9455(12)
α (deg)	90.466(3)				118.039(1)
β (deg)	102.738(3)	101.025(2)		101.912(7)	105.782(1)
γ (deg)	101.102(3)				92.554(1)
V (Å^3)	639.8(2)	1606.7(4)	3062.6(5)	4745(5)	1815.8(4)
Z	2	4	8	4	2
T (K)	296(2)	296(2)	296(2)	296(2)	296(2)
ρ_{calc} (g/cm^3)	1.289	2.032	2.132	2.064	1.864
$F(000)$	260.0	920.0	1840.0	2760.0	960.0
μ (Mo Kα, mm^{-1})	0.081	10.518	11.036	10.685	9.315
total reflns	4770	12 020	6854	18 162	13 017
unique reflns	2358	2985	1875	4544	6528
no. of observations	1432	2349	1648	3405	5330
no. of params	172	199	101	333	415
R_1[a]	0.0424	0.0284	0.0254	0.0482	0.0273
wR_2[b]	0.1167	0.0716	0.0532	0.1327	0.0656
GOF[c]	1.019	1.030	1.063	1.074	1.083

[a] $R_1 = \sum||F_o| - |F_c||/\sum|F_o|$. [b] $wR_2 = \{\sum w(F_o^2 - F_c^2)^2/\sum w(F_o^2)^2\}^{1/2}$. [c] GOF = $\{\sum w(F_o^2 - F_c^2)^2/(n-p)\}^{1/2}$, where n = number of reflections and p = total numbers of parameters refined.

chloride (80 mmol) was added dropwise within 20 min, and the solution was stirred at room temperature for 60 h. The resulting solution was added to 500 mL of 10% aq K_2CO_3, and the mixture was further stirred at room temperature for 1 h. The mixture was then extracted with CH_2Cl_2 (3 × 50 mL). The combined organic layers were washed with saturated $NaHCO_3$ (500 mL) and NaCl (500 mL), respectively, and dried with anhydrous $MgSO_4$, and the solvent was removed in vacuo to yield the crude product. Purification by silica gel chromatography using 100−200 mesh ZCX II eluted by petroleum ether−ethyl acetate (1:2, v/v) gave compound **1** (4.52 g, 91%). Anal. Calcd. for $C_{15}H_{12}N_4$: C, 72.56; H, 4.87; N, 22.57. Found: C, 72.57; H, 4.68; N, 22.75. IR (KBr disk): 2960 (w), 2918 (w), 2857 (w), 2232 (m), 1596 (s), 1472 (w), 1446 (m), 1407 (m), 1350 (m), 1226 (m), 989 (m), 926 (w), 861 (m), 784 (m), 479(m) cm^{-1}. ^{1}H NMR (400 MHz, $CDCl_3$): δ 8.63 (d, J = 4 Hz, 2H, ArH), 7.54 (s, 2H, ArH), 7.34 (d, J = 4 Hz, 2H, ArH), 2.75 (t, J = 8 Hz, 4H, CH_2), 2.03 (q, J = 8 Hz, 2H, CH_2).

Preparation of $[PbL^{2-}]_n$ (2). A mixture of $Pb(Ac)_2$ $3H_2O$ (38 mg, 0.1 mmol), BPCP ligand (25 mg, 0.1 mmol), and pyridine/H_2O/EtOH (1/1/1, 5 mL) was sealed in a 23 mL Teflon-lined stainless steel container and heated at 130 °C for 5 days, then cooled to room temperature at a rate of 1.5 °C·h^{-1}. The colorless prisms of **2** were collected and washed with EtOH and dried in air. Yield: 32 mg (65%, based on Pb). Anal. Calcd. for $C_{15}H_{12}N_2O_4Pb$: C, 36.66; H, 2.46; N, 5.70. Found: C, 36.39; H, 2.33; N, 5.92. IR (KBr disk): 2964 (w), 2915 (w), 2856 (w), 1597 (s), 1553 (m), 1472 (w), 1447 (m), 1406 (m), 1352 (m), 1226(m), 987 (m), 926 (w), 860 (m), 784 (m), 478 (m) cm^{-1}.

Preparation of $[PbL^{2-}]_n$ (3). A mixture of $Pb(Ac)_2$ $3H_2O$ (38 mg, 0.1 mmol), BPCP ligand (25 mg, 0.1 mmol), 4,4′-bipyridine (9 mg, 0.05 mmol), and pyridine/H_2O/EtOH (1/1/1, 5 mL) was sealed in a 23 mL Teflon-lined stainless steel container and heated at 130 °C for 5 days, then cooled to room temperature at a rate of 1.5 °C·h^{-1}. The colorless blocks of **3** were collected and washed with EtOH and dried in air. Yield: 27 mg (53%, based on Pb). Anal. Calcd. for $C_{15}H_{12}N_2O_4Pb$: C, 36.66; H, 2.46; N, 5.70. Found: C, 36.49; H, 2.83; N, 5.90. IR (KBr disk): 2962 (w), 2912 (w), 2850 (w), 1594 (s), 1553 (m), 1470 (w), 1442 (m), 1403 (m), 1355 (m), 1221 (m), 980 (m), 919 (w), 862 (m), 780 (m), 460 (m) cm^{-1}.

Preparation of $[Pb_3L^{2-}_3]_n$ (4). A mixture of $Pb(Ac)_2$ $3H_2O$ (38 mg, 0.1 mmol), BPCP ligand (25 mg, 0.1 mmol), and pyridine/H_2O/EtOH (1/1/1, 5 mL) was sealed in a 23 mL Teflon-lined stainless steel container and heated at 130 °C for 5 days, then cooled to room temperature at a rate of 15 °C·h^{-1}. The colorless prisms of **4** were collected and washed with EtOH and dried in air. Yield: 30 mg (60%, based on Pb). Anal. Calcd. for $C_{45}H_{36}N_6O_{12}Pb_3$: C, 36.66; H, 2.46; N, 5.70. Found: C, 36.58; H, 2.53; N, 5.90. IR (KBr disk): 2960 (w), 2916 (w), 2855 (w), 1595 (s), 1559 (m), 1475 (w), 1449 (m), 1404 (m), 1350 (m), 1222 (m), 980 (m), 921 (w), 860 (m), 782 (m), 470 (m) cm^{-1}.

Preparation of $[(Pb_2L^{2-}_2)\cdot 2H_2O]_n$ (5). A mixture of $Pb(Ac)_2$ $3H_2O$ (38 mg, 0.1 mmol), BPCP ligand (25 mg, 0.1 mmol), 4,4′-bipyridine (9 mg, 0.05 mmol) (11 mg, 0.05 mmol), and pyridine/H_2O/EtOH (1/1/1, 5 mL) was sealed in a 23 mL Teflon-lined stainless steel container and heated at 160 °C for 5 days, then cooled to room temperature at a rate of 1.5 °C·h^{-1}. The colorless blocks of **5** were collected and washed with EtOH and dried in air. Yield: 33 mg (67%, based on Pb). Anal. Calcd. for $C_{30}H_{28}N_4O_{10}Pb_2$: C, 35.36; H, 2.77; N, 5.50. Found: C, 35.31; H, 2.93; N, 5.72. IR (KBr disk): 3339 (m), 2952 (w), 2910 (w), 2840 (w), 1584 (s), 1548 (m), 1468 (w), 1440 (m), 1400 (m), 1352 (m), 1221 (m), 978 (m), 919 (w), 866 (m), 781 (m), 450 (m) cm^{-1}.

X-ray Crystal Structure Determination. Crystallographic data of **1−5** were collected at 296 K on a Bruker Smart APEXII-CCD Area Detector instrument with Mo Kα monochromated radiation (λ = 0.71073 Å) using the ω−φ scan technique. Data were reduced using SAINTPLUS, and an empirical absorption correction was applied using the SADABS program. The crystal structures were solved by the direct method[19] refined on F^2 by full-matrix least-squares using anisotropic displacement parameters for all non-hydrogen atoms. All the H atoms in **1−5** were introduced at the calculated positions and included in the structure-factor calculations. All the calculations were performed on a Dell workstation using the SHELXTL-97 crystallographic software package. A summary of key crystallographic information for **1−5** is given in Table 1. CCDC 872267 (**1**),

dx.doi.org/10.1021/cg300900m | Cryst. Growth Des. 2012, 12, 5338−5348

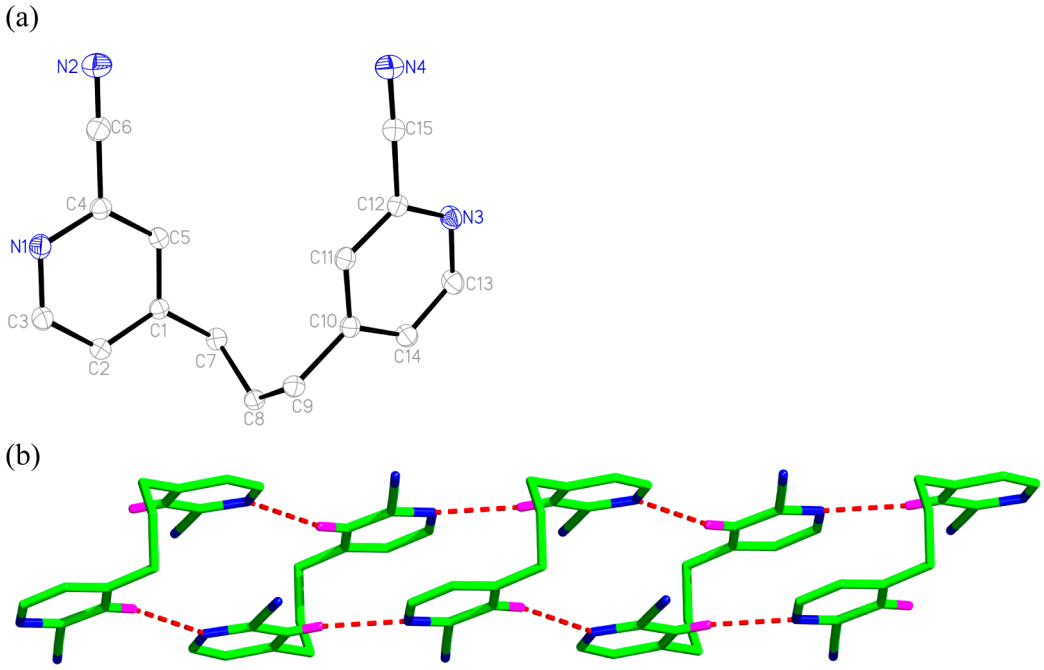

Figure 1. (a) View of the molecular structure of BPCP (**1**). (b) View of the one-dimensional chain structure formed via H-bonding interactions in **1** extending along the *c* axis. Atom color codes: H, pink; N, blue; and C, green. All H atoms except those related to H-bonding interactions were omitted for clarity.

872268 (**2**), 872271 (**3**), 872269 (**4**), and 872278 (**5**) contain the supplementary crystallographic data. These data can be obtained free of charge via www.ccdc.cam.ac.uk/conts/retrieving.html (or from the Cambridge Crystallographic Data Center, 12 Union Road, Cambridge CB2 1EZ, U.K.; fax: (44) 1223 336-033. E-mail: deposit@ccdc.cam.ac.uk). Selected bond lengths and angles for **2**−**5** are listed in Table S1 (see Table S1 in the Supporting Information).

RESULTS AND DISCUSSION

Synthetic and Spectral Aspects. Reactions of 1,3-bis(4-pyridyl)propane-*N*,*N*′-dioxide with 10 equiv of $(Me)_3SiCN$ and 4 equiv of benzoyl chloride in CH_2Cl_2 produced a new flexible 1,3-bis(4-pyridyl-3-cyano)propane (**1**) in 91% yield (Scheme 1).

Recent studies have revealed that the in situ ligand transformation reaction may occur during hydro(solvo)thermal reactions, which is currently regarded as a feasible and effective strategy to obtain novel CPs that are inaccessible or not easily achieved by the conventional methods.[20] However, the controlled synthesis of supramolecular isomers is still a major challenge.[5] Small changes in one or more of the variables of hydrothermal reactions, such as reaction temperature, pH value, duration, and the presence of other contributing additives, either the solvent or other species, have a profound influence on the crystallization outcome.[7c,21] As far as these factors are concerned, polymorphs **2**−**4** and their polymorphic frameworks **5** were successfully obtained by in situ reaction of BPCP with Pb(II) acetate through tuning the solvothermally temperature, reaction cooling rate, and additive. According to our experimental results, the polymorphs **3** and **2** were solvothermally prepared from Pb(II) acetate and the BPCP ligand in the presence of 4,4′-bipyridine, or not, at 130 °C, respectively. Interestingly, although 4,4′-bipyridine does not participate in the structure construction, we cannot obtain the product **3** without the addition of 4,4′-bipyridine. This fact strongly suggests that the additive can effectively promote the formation of different superstructures. A similar phenomenon is observed in the reports by Tong[7c] and Hu.[21a] The preparation of polymorph **4** is similar to that of polymorph **2**, except that the cooling rate of 1.5 °C·h^{-1} was replaced by 15 °C·h^{-1}. Notably, when the reaction temperature was raised up to 160 °C, complex **5** was generated through the similar manner to that described for **3**. Significantly, the use of pyridine to adjust the pH value of the reaction systems is another key point for the crystallization of **2**−**5**, and when other basic reagents, such as NaOH, KOH, and 2,6-dimethylpyridine, were used instead, crystalline products suitable for X-ray diffraction could not be obtained under similar conditions.

Compounds **1**−**5** were stable toward oxygen and moisture. **1** was soluble in CH_3Cl, MeOH, DMF, and DMSO, but **2**−**5** were almost insoluble in common organic solvents. The elemental analyses of **1**−**5** were consistent with their chemical formula. The ^{1}H NMR spectrum of **1** in $CDCl_3$ exhibited one singlet and two doublet for the phenyl groups at 8.63 ppm (d, J = 4 Hz), 7.54 ppm (s), 7.34 ppm (d, J = 4 Hz), and the bridging methylene groups at 2.75 (t, J = 8 Hz), 2.03 (q, J = 8 Hz). In the IR spectra of **1**, the strong bands at 2232 cm^{-1} were assigned to be the C≡N stretching vibration.[22] The IR spectra of **2**−**5** showed peaks in the range of 1548−1559 and 1468−1474 cm^{-1}, suggesting that the C≡N groups hydrolyzed to COOH groups.[23] The strong peaks at about 860 cm^{-1}, and middle peaks in the range of 449−477 cm^{-1}, mean the existence of pyridyl groups in the complexes **1**−**5**.[24] The PXRD patterns of **2**−**5** were matched with the simulated patterns generated from their single-crystal data (see the Supporting Information, Figure S1).

Crystal Structure of 1. Compound **1** crystallizes in the triclinic space group $P\bar{1}$,and its asymmetric unit contains one BPCP molecule (Figure 1a). As shown in Figure 1b, the N atoms of the pyridyl groups interact with the H atoms of the pyridyl groups with C5 and C11 [C5···N3 (1 − x, 1 − y, 1/2 − z); C11···N1 (1 − x, 1 − y, 1 − z)] to afford intermolecular

dx.doi.org/10.1021/cg300900m | *Cryst. Growth Des.* 2012, 12, 5338−5348

hydrogen bonds, forming a 1D chain extending along the *c* axis (Figure 1b).

Crystal Structure of 2. Polymorph **2** crystallizes in the monoclinic space group $P2_1/c$, and its asymmetric unit contains one PbL^{2-} unit. Each Pb atom adopts a distorted octahedral geometry and is coordinated by four O atoms of four bridging carboxylate groups from four different L^{2-} ligands and two N atoms from two L^{2-} ligands (Figure 2a). The mean Pb−O bond length (2.582(4) Å) is shorter than that of $[Pb(pydc)]_n$ (H_2pydc = pyridine-2,6-dicarboxylic acid (2.648(8) Å), while the mean Pb−N bond length (2.512(4) Å) is shorter than that in $[Pb(pydc)]_n$ (2.486(3) Å).[25] The L^{2-} ligand in **2** only takes TT conformation (Scheme 2a), and the carboxylate groups display μ_2-η^1:η^1- or μ_2-η^2-bridged modes. Thus, each L^{2-} ligand in **2** acts as a μ_4-bridge to link four Pb(II) atoms. Pb1 and its symmetry-related Pb1A are bridged by two L^{2-} ligands to generate a dinuclear $[Pb_2L^{2-}{}_2]$ ringlike unit with an approximate diameter of 6.41 Å (between C8 and C8A) × 13.42 Å (between Pb1 and Pb1A) (Figure 2b). Each Pb1 atom in the $[Pb_2L^{2-}{}_2]$ unit interconnects its equivalent ones via bridging carboxylate groups to form a 1D $[Pb_2L^{2-}{}_2]_n$ double chain extending along the *c* axis (Figure 2c). One pair of rings (green and cyan) is arranged in an almost vertical way. The aforementioned 1D double chains are further connected to adjacent ones by Pb1 atoms, leading to a 2D ladder-like structure in the *ac* plane (see the Supporting Information, Figure S2). Each 2D structure is further connected by carboxylate groups to generate a 3D porous structure with 1D channels (6.64 Å × 11.34 Å) running along the *c* axis (Figure 2d). The effective solvent accessible volume of 163.7 $Å^3$ per unit cell (10.2% of the total cell volume calculated by the Platon program) is filled with guest molecules.[26] A better insight into the nature of **2** can be achieved by the application of a topological approach, namely, reducing multidimensional structures to simple node-and-linker nets. As discussed above, the L^{2-} ligands act as 3-connected nodes and Pb(II) centers act as 6-connected nodes. In this way, the resulting structure of **2** is symbolized as a (3,6)-connected $(4\cdot5^2)(4^2\cdot5^2\cdot6^7\cdot7^3\cdot8)$ topology (Figure 2e).

Crystal Structure of 3. For polymorph **3**, there are the same components as that of **2** in the fundamental unit (Figure 3a), however, the L^{2-} ligand takes a different conformation, TT″ (Scheme 2c), and the two carboxylate groups display the same μ_2-η^1:η^1-bridged modes, which are distinguished from that of **2**. Herein, different from that of **2**, first, **3** crystallizes in the orthorhombic space group *Fdd*2, and its asymmetric unit only contains half a PbL^{2-} unit. Second, different from that of **2**, the structural feature of **3** is that Pb1 and Pb1A are linked by one L^{2-} ligand to afford a $[Pb_2L^{2-}]$ semi-ring-like unit. Each Pb1 atom in the $[Pb_2L^{2-}]$ unit interconnects its equivalent ones via bridging carboxylate groups to form a 1D $[Pb_2L^{2-}]_n$ chain along the *b* axis (see the Supporting Information, Figure S3). Moreover, each 1D chain is connected to neighboring ones by Pb1 atoms to afford a 2D sheet in the *ab* plane with square meshes (12.18 Å × 12.18 Å) (Figure 3b). Finally, different from that of **2**, the different packing mode in **3** is that the 2D layers are further connected by L^{2-} bridges to generate a 3D framework with 1D channels (11.11 Å × 12.18 Å) running along the *c* axis (Figure 3c). The bridging ligands are located in the 1D channels, so there is still approximately 3.7% of the crystal volume to be filled by solvent molecules, which is much lower than that of **2**. Topologically, both L^{2-} ligands and Pb

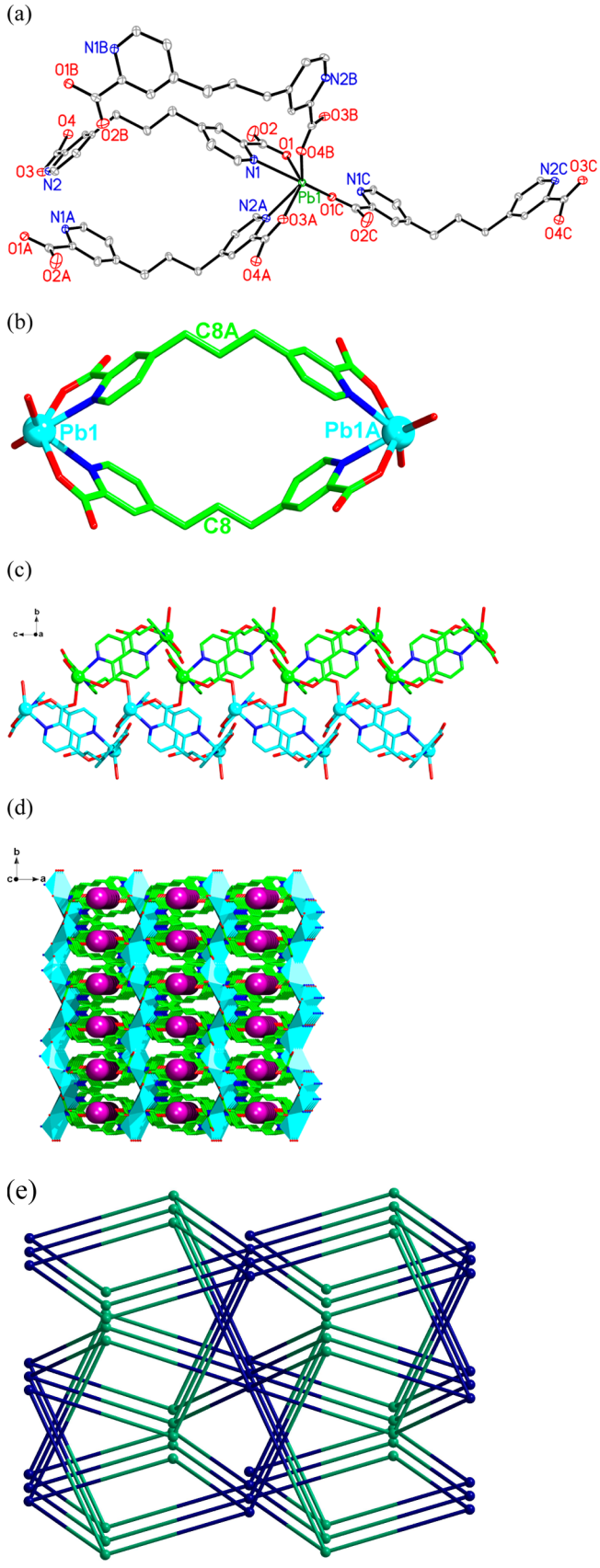

Figure 2. (a) View of the coordination environments of the Pb1 center in **2** with labeling schemes. Symmetry codes: (A) $-x + 1, -y + 1, -z + 1$; (B) $-x + 1, y - 1/2, -z + 1/2$; (C) $-x, -y + 1, -z$. (b) View of one dinuclear $[Pb_2L^{2-}{}_2]$ ringlike unit of **2**. Symmetry codes: (A) $-x + 1, -y + 1, -z + 1$. (c) View of a section of the 1D double chain

dx.doi.org/10.1021/cg300900m | *Cryst. Growth Des.* 2012, 12, 5338−5348

Figure 2. continued

extending along the *c* axis. (d) View of a 3D porous structure in **2** along the *c* axis. (e) Topological view showing the equivalent 3D framework of **2**. The purple pillars represent the 1D channel in **2**. Atom color codes: Pb, cyan; O, red; N, blue; and C, green. All hydrogen atoms are omitted for clarity.

atoms act as a 4-connected node, and thus the 3D structure of **3** can be rationalized as a $(6^6)_2$ net (Figure 3d).

Crystal Structure of 4. For polymorph **4**, there are the same components as that of **2** and **3** in the fundamental unit, which crystallizes in the monoclinic space group *C*2/*m*, and its asymmetric unit contains half a $Pb_3L^{2-}{}_3$ unit. As shown in Figure S4 (see the Supporting Information), the Pb atoms in **4** adopt two different coordination geometries. Both Pb1 and Pb2 are seven-coordinated, each coordinated by six O atoms of four bridging carboxylate groups from four different L^{2-} ligands and one N atom from one L^{2-} ligand, to complete a pentagonal bipyrimidal coordination environment (see the Supporting Information, Figure S4a,b). The mean Pb1−O bond length (2.621(5) Å) is longer than that of $\{[Pb_6(pydc)_6]\cdot H_2O\}_n$ (2.529(7) Å), while the Pb1−N bond length (2.514(10) Å) is longer than that in $\{[Pb_6(pydc)_6]\cdot H_2O\}_n$ (2.492(3) Å).[27] The mean Pb2−O bond length (2.637(3) Å) is shorter than that of $[Pb(dpaea)(H_2O)]_2\cdot[Pb(dpaea)]\cdot 6H_2O$ (H_2dpaea = *N*,*N*-bis[(6-carboxypyridin-2-yl)methyl]ethylamine, 2.467(2) Å).[28] Pb3 is eight-coordinated by four O atoms of four bridging carboxylate groups and four N atoms from four different L^{2-} ligands (see the Supporting Information, Figure S4c), and the coordination geometry around Pb3 may be described as a distorted trigonal dodecahedron. The mean Pb3−O and Pb3−N bond lengths (2.715(5) vs 2.662(1) Å) are shorter than those of the corresponding ones in $[Pb(pydc)]_n$ (2.612(8) vs 2.692(2) Å).[29] In **4**, the Pb−N and Pb−O bond lengths fall in the ranges of 2.361(8)−2.829(8) and 2.491(13)−2.669(14) Å, respectively, which are comparable to the previously reported values.[30] The L^{2-} ligand in **4** takes conformations TT and TT′ (Scheme 2a,b), and the carboxylate groups display μ_2-η^2:η^1- or μ_2-η^2-bridged modes.

In **4**, Pb3 and Pb3A atoms are linked by two L^{2-} ligands to form a dinuclear ringlike $[Pb_2L^{2-}{}_2]$ unit with a rough diameter of 5.92 Å (between C23 and C23A) × 14.04 Å (between Pb3 and Pb3A), similar to that observed in **2** (Figure 4a). Each Pb3 atom in the $[Pb_2L^{2-}{}_2]$ unit interconnects its equivalent ones via bridging carboxylate groups to form a 1D $[Pb_2L^{2-}{}_2]_n$ chain along the *a* axis (Figure 4b). Such 1D chains are linked by Pb1 and Pb2 atoms to afford a 2D network with rectangular grids (6.09 × 10.84 Å) in the *ab* plane (Figure 4c). Other L^{2-} ligands act as a pillar to link the adjacent 2D networks to form a 3D framework with dimensions of 10.84 × 14.86 × 19.59 $Å^3$ along the *ac* plane (Figure 4d). This framework was big enough to allow the other net to penetrate to form a 2-fold interpenetrating framework, which can be described as a trinodal (3,6,10)-connected topology with a point symbol of (4^3)-$(4^4\cdot6^{10}\cdot8)(4^8\cdot6^{24}\cdot8^9\cdot10^4)$ (Figure 4e). The Platon program analysis suggests that approximately 12.7% (**4**) of the crystal volume is accessible to the solvents, which is a little higher than that of **2** (10.2%).

Crystal Structure of 5. Complex **5** crystallizes in the triclinic space group $P\bar{1}$, and its asymmetric unit contains one $Pb_2L^{2-}{}_2$ unit and two H_2O molecules. As shown in Figure 5a,b, each Pb atom in **5** is eight-coordinated by two nitrogen atoms

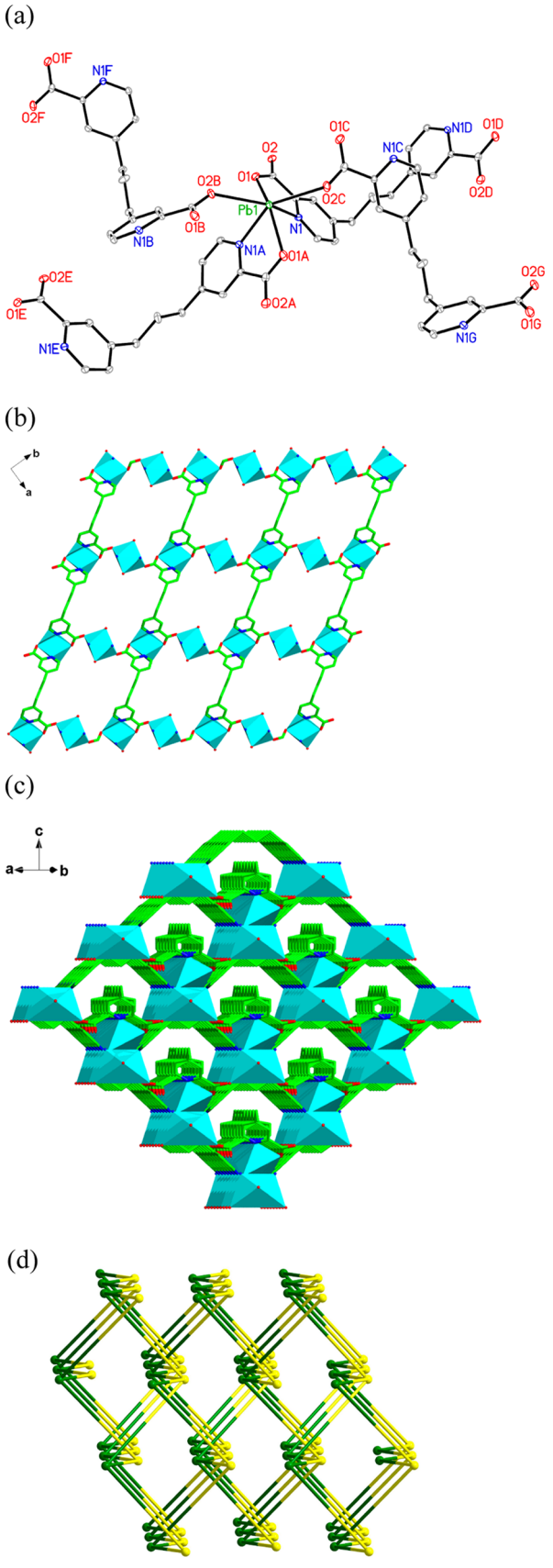

Figure 3. (a) View of the coordination environments of the Pb1 center in **3** with labeling schemes. Symmetry codes: (A) −*x*, −*y* − 1, −*z*; (B) −*x* + 1/4, *y* − 1/4, *z* − 1/4; (C) *x* − 1/4, −*y* − 3/4, *z* − 1/4; (D) −*x* − 1/2, −*y* − 1/2, *z*; (E) *x* + 1/2, *y* − 1/2, *z*; (F) *x* + 3/4, −*y* − 3/4, *z*

dx.doi.org/10.1021/cg300900m | *Cryst. Growth Des.* 2012, 12, 5338−5348

Figure 3. continued

− 1/4; (G) $-x - 3/4, y - 1/4, z - 1/4$. (b) View of a 2D sheet in **3** extending along the *ab* plane. (c) View of a 3D framework in **3** along the *b* axis. (d) Topological view showing the equivalent 3D framework of **3**. Atom color codes: Pb, cyan; O, red; N, blue; and C, green. All hydrogen atoms are omitted for clarity.

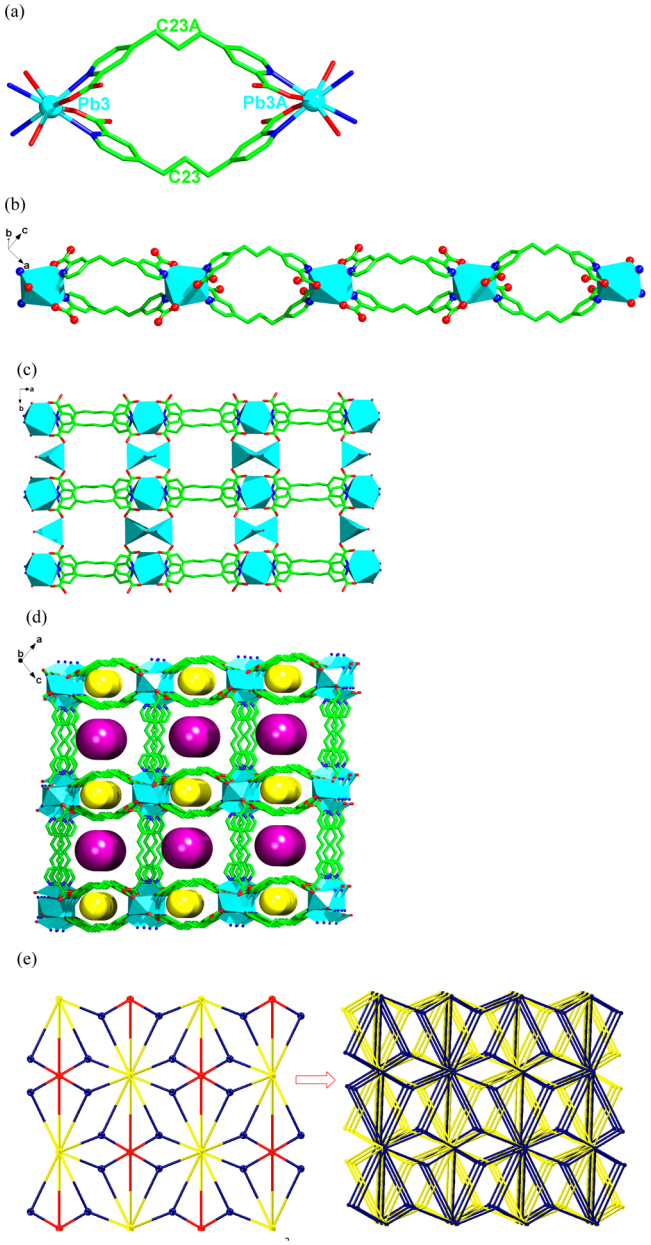

Figure 4. (a) View of one dinuclear $[Pb_2L^{2-}{}_2]$ ringlike unit of **4**. Symmetry codes: (A) $-x + 5/2, -y + 1/2, -z$. (b) View of a section of the 1D chain along the *c* axis. (c) View of a 2D network in **4** along the *ab* plane. (d) View of a 3D framework in **4** along the *b* axis. The purple and yellow pillars represent 1D channels in **4**. (e) Schematic representation of the trinodal (3,6,10)-connected topology with a point symbol of $(4^3)(4^4{\cdot}6^{10}{\cdot}8)(4^8{\cdot}6^{24}{\cdot}8^9{\cdot}10^4)$. Atom color codes: Pb, cyan; O, red; N, blue; and C, green. All hydrogen atoms are omitted for clarity.

from two L^{2-} ligands, five carboxylate oxygen atoms from four different L^{2-} ligands, and one coordinated water molecule, and thus the coordination geometry around Pb may be described a distorted trigonal dodecahedron. The mean Pb1−O and Pb1−N bond lengths (2.682(2) vs 2.597(1) Å) are longer than those of the corresponding ones in **4** (2.657(2) vs 2.588(1) Å). The average Pb2−O and Pb2−N bond length (2.758(3) vs 2.600(5) Å) is longer than that of $[Pb(HOIP)(pyc)_2]_2$ (2.460(5) vs 2.563(5) Å; HOIP = 2-(4-hydroxylbenzene) imidazo[4,5-*f*]1,10-phenanthroline, Hpyc = pyridyl-2-carboxylic acid).[31] The L^{2-} ligand in **5** takes conformations TT′ and TG″ (Scheme 2b,f), and the carboxylate groups display μ_2-η^2:η^1- or μ_2-η^2-bridged modes. As shown in Figure 5c,d, it was interesting that there existed two kinds of dinuclear $[Pb_2L^{2-}{}_2]$ units in **5**. One of the dinuclear $[Pb_2L^{2-}{}_2]$ units showed a little flat ring with a rough diameter of 5.75 Å (between C23 and C23A) × 14.04 Å (between Pb2 and Pb2A) (Figure 5c). Another displayed a distorted ring with an approximate 6.32 Å (between C9 and C9A) × 12.54 Å (between Pb1 and Pb1A) (Figure 5d). These two $[Pb_2L^{2-}{}_2]$ units are interconnected by bridging carboxylate groups in a alternate fashion to form a 1D $[Pb_2L^{2-}{}_2]_n$ ladder-like chain (Figure 5e). Such 1D chains are further linked to its adjacent ones by Pb1 and Pb2 atoms to afford a 2D undulant network with a 6-connected $(3^6{\cdot}4^6{\cdot}5^3)$ topology (Figure 5e−g). The weak interactions (2.925(2) Å) between Pb2 and O9 and the hydrogen-bonding interactions [C4−H4···O9, 2.583(5) (Å)] between O atoms of H_2O molecules (O9) in one network and H atoms of pyridine rings in the adjacent network connect the 2D networks to afford a 3D framework with 1D channels (4.20 Å × 7.50 Å) looking along the *c* axis. There is still approximately 19.9% of the crystal volume to be filled by solvent molecules, which is much higher than that of **2**−**4**.

Effects of Reaction Conditions and Conformations of Ligand on the Formation of Four Coordination Polymers. Polymorphism, which can be considered a specific subset of supramolecular isomerism, is particularly rare for coordination polymers.[7] To the best of our knowledge, there is only one case reported about the polymorphs constructed from a single flexible linked dicarboxylate as the building block materials.[6a] Fortunately, the present study shows that the new flexible ligand, BPCP, can also act as a convenient building block for the construction of novel CPs, whose syntheses can be easily accomplished by solvothermal reactions. During the preparation of four novel coordination polymers, process temperature, cooling rate, and additive are three key factors in controlling the topologies of CPs. For example, by fine-tuning the reaction temperature to 130 and 160 °C, complexes **3** and **5** have been synthesized, respectively. Complex **3** possesses a 3D metal−organic framework with a 1D channel (11.11 Å × 12.18 Å), in which dinuclear semi-ring-like $[Pb_2L^{2-}]$ units are bridged by L^{2-} ligands. Complex **5** features a 3D supramolecualr architecture constructed from 2D undulant layer motifs joined by hydrogen-bonding interactions and weak interactions. The difference of the bridging mode and the conformation of L^{2-} ligands in the two complexes must be induced by different reaction temperatures, which should be mainly responsible for the different architectures of **3** and **5**. The L^{2-} ligand in **3** adopts a μ_4-bridging mode and TT″ conformation to link Pb(II) centers, resulting in a dinuclear semi-ring-like $[Pb_2L^{2-}]$ unit. The L^{2-} ligand in **5** takes a μ_4-bridging mode and TT′ and TG″ conformations to connect Pb(II) atoms, leading to two dinuclear ringlike $[Pb_2L^{2-}{}_2]$ units. Thus, this result reveals that, for a more flexible ligand, the assembly will be more dependent on the temperature. Comparing polymorph **2** with **3**, the addition of 4,4′-bipyridine

dx.doi.org/10.1021/cg300900m | *Cryst. Growth Des.* 2012, 12, 5338−5348

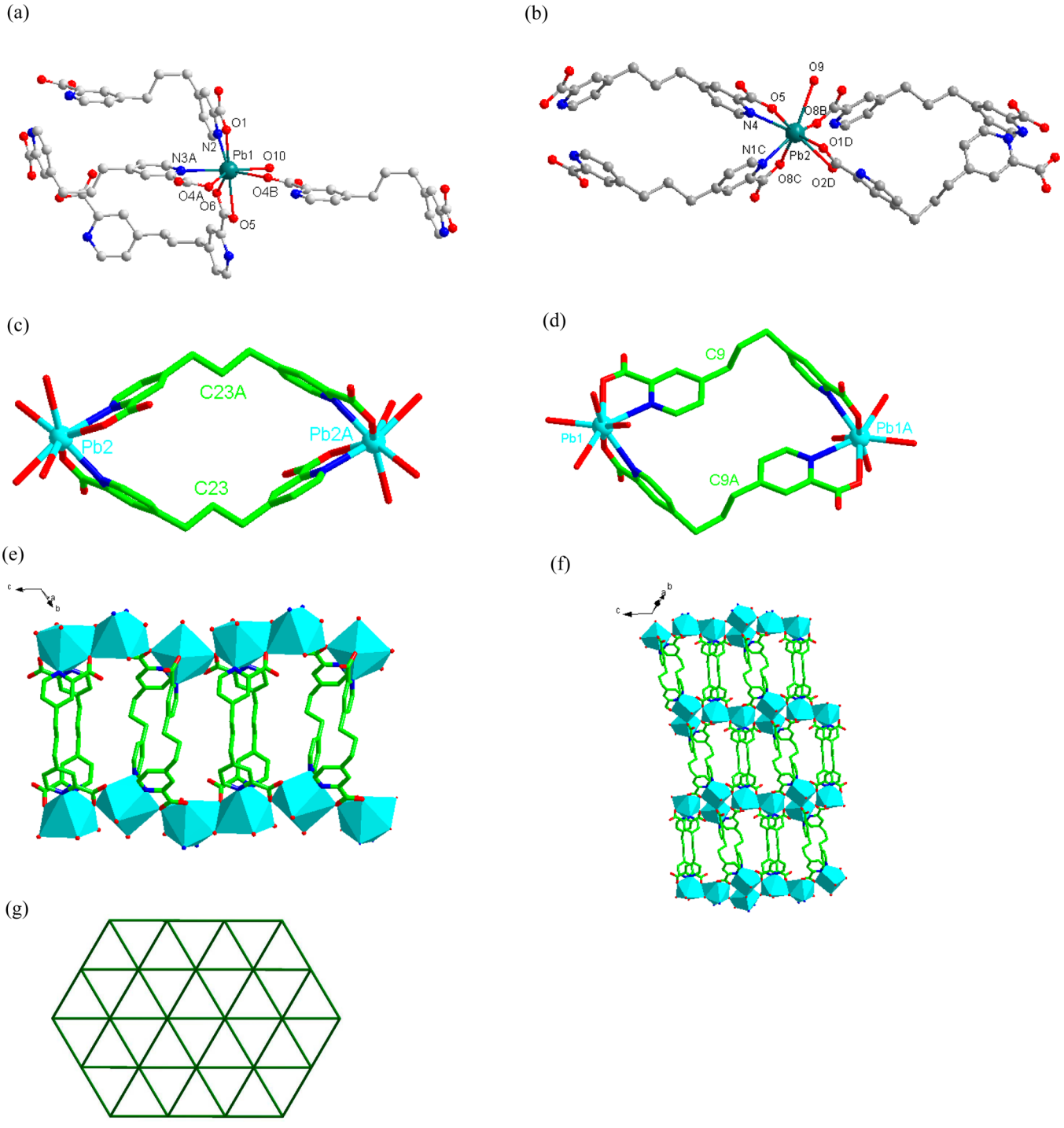

Figure 5. (a, b) View of the coordination environments of Pb centers in **5** with labeling schemes. Symmetry codes: (A) $-x + 1, -y + 2, -z + 2$; (B) $x - 1, y - 1, z - 1$; (C) $-x + 1, -y + 2, -z + 1$; (D) $-x, -y + 1, -z + 1$. (c) View of one dinuclear $[Pb_2L^{2-}{}_2]$ ringlike unit of **5**. (d) View of one distorted dinuclear $[Pb_2L^{2-}{}_2]$ ringlike unit of **5**. (e) View of a section of the 1D ladder-like chain along the *c* axis. (f) View of a 2D network in **5** in the *bc* plane. (g) A schematic representation of the 6-connected $(3^6{\cdot}4^6{\cdot}5^3)$ topology. The red dashed lines represent hydrogen-bonding interactions. Atom color codes: Pb, cyan; O, red; N, blue; and C, green.

promotes the formation of **3** under similar reaction conditions. A similar phenomenon can be documented by recent reports by Tong[7c] and Hu.[21a] Thus, this fact strongly suggests that the additive can effectively promote the formation of different superstructures. Additionally, the preparation of polymorph **4** is similar to that of polymorph **2**, except that the cooling rate of 1.5 °C·h^{-1} was replaced by 15 °C·h^{-1}. The result demonstrates that this crystallization condition can also play another important role in the formation of complexes. To our knowledge, there is no case reported about the polymorphs constructed from a subtle difference in cooling rate as a dominant structural factor.

Photoluminescence Properties. The photoluminescent properties of **1**−**5** and H_2L in the solid state at room temperature were studied. The result demonstrated that the BPCP ligand (**1**) did not show photoluminescent properties.

dx.doi.org/10.1021/cg300900m | *Cryst. Growth Des.* 2012, 12, 5338−5348

The emission spectra of supramolecular isomers **2**–**5** and the H_2L ligand are very similar, as shown in Figure 6. Upon

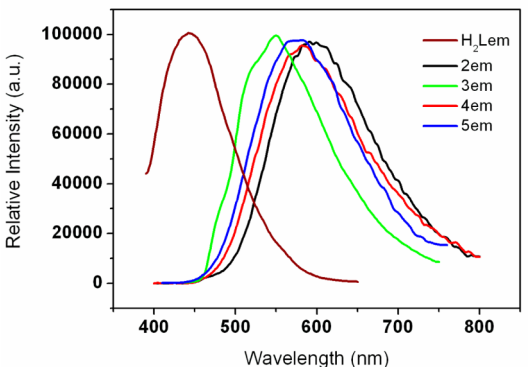

Figure 6. Emission spectra of **2**–**5** in the solid state at ambient temperature.

excitation at 371 nm, the strongest emission peak for the free H_2L ligand appears at 435 nm, corresponding to the n → π^* transitions. For **2**–**5**, excitation of the microcrystalline samples at 384, 387, 378, 363, and 351 nm leads to the generation of intense fluorescent emissions (Figure 6), with similar maximum peaks observed in the blue region (**2**, 543 nm; **3**, 535 nm; **4**, 520 nm; and **5**, 540 nm), which may be attributed to the ligand-centered π → π^* electronic transitions.[32] The different emission bands of compounds **2**–**5** may be assigned to the coordination diversities of the Pb(II) ion centers and the rigid differences of these Pb(II) coordination frameworks.

Thermogravimetric Analysis. To investigate the thermal stability of **2**–**5**, TGA and DSC experiments were performed for these materials under a N_2 atmosphere. As depicted in Figure 7, the thermograms of polymorphs **2**–**4** show similar

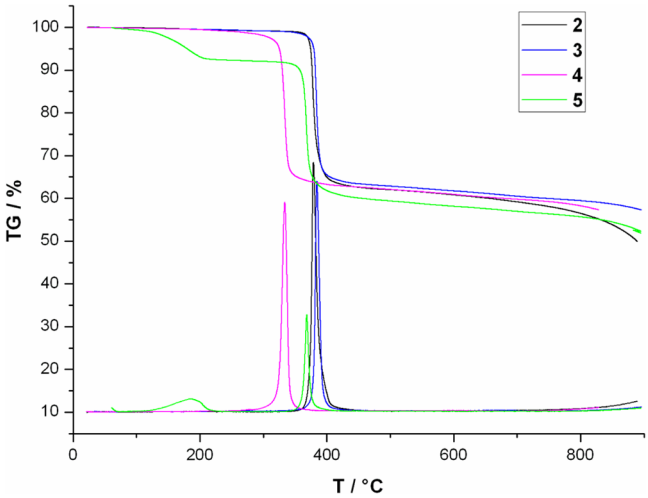

Figure 7. TGA and DSC curves of compounds **2**–**4**.

profiles. The three polymorphs are thermally very stable up to 312 °C. Because there are no solvent molecules in the frameworks, there is a plateau region ranging from 25 to 390 °C in **2**, 393 °C in **3**, and 312 °C in **4**, followed by a sudden decrease in the weight, suggesting the onset of the decomposition temperature of the complexes. This can be confirmed by DSC analysis. The DSC curves show an endothermic peak, corresponding to the decomposition process. The final residue of ca. 54.3, 54.9, and 54.7% for polymorphs **2**–**4**, respectively, is in agreement with the percentage of $PbCO_3$ in all cases (calcd. 54.5%), as observed in the previous studies.[32a,33] The TGA of **5** exhibits two main steps of weight loss. A weight loss of 6.1% in the temperature range of 50–119 °C shows the release of all guest water molecules (calcd. 3.5%). The second step of weight loss from 378 °C corresponds to the thermal decomposition of the organic groups. The final residue of ca. 49.3% is in agreement with the percentage of $PbCO_3$ in **5** (calcd. 48.9%). In addition, the weight loss, being an endothermic process, occurred at ca. 119 °C for **5**, 312 °C for **4**, 390 °C for **2**, and 393 °C for **3**, implying an increase in thermal stability from compounds **5**, **4**, **2**, and to **3**.

CONCLUSIONS

In conclusion, three novel true polymorphous CPs and one of their polymorphic frameworks were successfully synthesized employing the same ratio of reaction materials, containing a new flexible linker BPCP with a relatively long spacer, via an in situ ligand transformation reaction, cooperating with fine control over synthetic conditions. The structural results show that utilizing the flexible ligands is a deliberate strategy to achieve diversity in CP structures, which may help chemists obtain new polymorphs. Analyses of synthetic conditions, structures, and coordination modes of the L^{2-} ligand reveal that reaction temperature, cooling rate, and additive are three key factors to products and coordination conformation of the L^{2-} ligand . The L^{2-} ligands in **2**–**5** adopt a μ_4-bridging mode, and a TT, TT′, TT″, or TG″ conformation, to link Pb(II) centers, resulting in a dinuclear ringlike $[Pb_2L^{2-}{}_2]$ unit in **2** and **4**, a dinuclear semi-ring-like $[Pb_2L^{2-}]$ unit in **3**, and two dinuclear ringlike $[Pb_2L^{2-}{}_2]$ units in **5**, respectively. Based on these different building units, polymorphs **2** and **4** display a 3D framework with 1D channels. Polymorph **3** features a 2-fold interpenetrating framework with a trinodal (3,6,10)-connected topology with a point symbol of $(4^3)(4^4{\cdot}6^{10}{\cdot}8)(4^8{\cdot}6^{24}{\cdot}8^9{\cdot}10^4)$. Polymorphic framework **5** exhibits a 3D supramolecualr architecture built up from 2D undulant layer motifs joined by hydrogen-bonding interactions and weak interactions. The differences in conformation and packing alignment should be mainly responsible for the different architectures of complexes **2**–**5**. Most importantly, the study also reveals that the structural differences of **2**–**5** result in the differences in photoluminescence properties. This work may provide a useful approach for the design and construction of other structural isomeric crystalline materials, which further helps us to understand the relationships between structures and properties.

ASSOCIATED CONTENT

Supporting Information

Table of selected bond lengths and angles for **2**–**5**, PXRD patterns for **2**–**5**, view of **2** along the *ac* plane, view of **3** along the *b* axis, and view of coordination environments of Pb centers in **4**. Crystal structure data for **1**–**5** in CIF format. This material is available free of charge via the Internet at http://pubs.acs.org.

AUTHOR INFORMATION

Corresponding Author

*E-mail: lyhxxjbm@126.com (B.-M.J.), dcx@zzu.edu.cn (C.D.).

Notes

The authors declare no competing financial interest.

■ ACKNOWLEDGMENTS

We are grateful to the Natural Science Foundation of China (Grant No.21072089) and the Science and Technology Innovation Team support programs of Henan Province University (No. 2012IRTSTHN019) for the financial support.

■ REFERENCES

(1) (a) Zhang, J.-P.; Huang, X.-C.; Chen, X.-M. *Chem. Soc. Rev.* **2009**, *38*, 2385. (b) Moulton, B.; Abourahma, H.; Bradner, M. W.; Lu, J.; McManus, G. J.; Zaworotko, M. J. *Chem. Commun.* **2003**, 1342. (c) Abourahma, H.; Moulton, B.; Kravtsov, V.; Zaworotko, M. J. *J. Am. Chem. Soc.* **2002**, *124*, 9990. (d) Moulton, B.; Zaworotko, M. J. *Chem. Rev.* **2001**, *101*, 1629.

(2) Caskey, S. R.; Wong-Foy, A. G.; Matzger, A. J. *Inorg. Chem.* **2008**, *47*, 7751.

(3) Allen, F. H. *Acta Crystallogr., Sect. B* **2002**, *58*, 380.

(4) (a) Brittain, H. G., Ed. *Polymorphism in Pharmaceutical Solids*; Marcel Dekker: New York, 1999. (b) Byrn, S. R.; Pfeiffer, R. R.; Stowell, J. G. *Solid State Chemistry of Drugs*, 2nd ed.; SSCI, Inc.: West Lafayette, IN, 1999. (c) Bernstein, J. *Polymorphism in Molecular Crystals*; Clarendon Press: Oxford, U.K., 2002. (d) Hilfiker, R., Ed. *Polymorphism in the Pharmaceutical Industry*; Wiley-VCH: Weinheim, Germany, 2006.

(5) (a) Li, D.-S.; Zhang, P.; Zhao, J.; Fang, Z.-F.; Du, M.; Zou, K.; Mu, Y.-Q. *Cryst. Growth Des.* **2012**, *12*, 1697. (b) Wu, Y.-P.; Li, D.-S.; Fu, F.; Dong, W.-W.; Zhao, J.; Zou, K.; Wang, Y.-Y. *Cryst. Growth Des.* **2011**, *11*, 3850. (c) Nauha, E.; Ojala, A.; Nissinen, M.; Saxell, H. *CrystEngComm* **2011**, *13*, 4956. (d) Han, L.; Zhao, W.; Zhou, Y.; Li, X.; Pan, J. *Cryst. Growth Des.* **2008**, *8*, 3504. (e) Zhang, J.-P.; Chen, X.-M. *Chem. Commun.* **2006**, 1689.

(6) (a) Yang, G.-P.; Hou, L.; Wang, Y.-Y.; Zhang, Y.-N.; Shi, Q.-Z.; Batten, S. R. *Cryst. Growth Des.* **2011**, *11*, 936. (b) Li, Z.-G.; Wang, G.-H.; Jia, H.-Q.; Hu, N.-H.; Xu, J.-W. *CrystEngComm* **2007**, *9*, 882. (c) Peng, Y.-F.; Ge, H.-Y.; Li, B.-Z.; Li, B.-L.; Zhang, Y. *Cryst. Growth Des.* **2006**, *6*, 994. (d) Gale, P. A.; Light, M. E.; Quesada, R. *Chem. Commun.* **2005**, 5864. (e) Li, B.; Peng, Y.; Li, B.; Zhang, Y. *Chem. Commun.* **2005**, 2333. (f) Huang, X.-C.; Zhang, J.-P.; Chen, X.-M. *J. Am. Chem. Soc.* **2004**, *126*, 13218. (g) Kumar, V. S. S.; Pigge, F. C.; Rath, N. P. *Cryst. Growth Des.* **2004**, *4*, 651. (h) Soldatov, D. V.; Ripmeester, J. A.; Shergina, S. I.; Sokolov, I. E.; Zanina, A. S.; Gromilov, S. A.; Dyadin, Y. A. *J. Am. Chem. Soc.* **1999**, *121*, 4197.

(7) (a) Hao, Z.-M.; Zhang, X.-M. *Cryst. Growth Des.* **2007**, *7*, 64. (b) Huang, X.-C.; Zhang, J.-P.; Lin, Y.-Y.; Chen, X.-M. *Chem. Commun.* **2005**, 2232. (c) Tong, M.-L.; Hu, S.; Wang, J.; Kitagawa, S.; Ng, S. W. *Cryst. Growth Des.* **2005**, *5*, 837. (d) Shin, D. M.; Lee, I. S.; Cho, D.; Chung, Y. K. *Inorg. Chem.* **2003**, *42*, 7722.

(8) (a) Bond, A. D.; Boese, R.; Desiraju, G. R. *Angew. Chem., Int. Ed.* **2007**, *46*, 618. (b) Jetti, R. K. R.; Boese, R.; Thallapally, P. K.; Desiraju, G. R. *Cryst. Growth Des.* **2003**, *3*, 1033.

(9) (a) Wang, Z.-W.; Ji, C.-C.; Li, J.; Guo, Z.-J.; Li, Y.-Z.; Zheng, H.-G. *Cryst. Growth Des.* **2009**, *9*, 475. (b) Mahata, P.; Natarajan, S. *Inorg. Chem.* **2007**, *46*, 1250. (c) Cao, R.; Sun, D. F.; Liang, Y. C.; Hong, M. C.; Tatsumi, K.; Shi, Q. *Inorg. Chem.* **2002**, *41*, 2087.

(10) (a) Sun, D.; Xu, H.-R.; Yang, C.-F.; Wei, Z.-H.; Zhang, N.; Huang, R.-B.; Zheng, L.-S. *Cryst. Growth Des.* **2010**, *10*, 4642. (b) Mahata, P.; Sen, D.; Natarajan, S. *Chem. Commun.* **2008**, 1278. (c) Zuhayra, M.; Kampen, W. U.; Henze, E.; Soti, Z.; Zsolnai, L.; Huttner, G.; Oberdorfer, F. A. *J. Am. Chem. Soc.* **2006**, *128*, 424. (d) Long, L.-S.; Wu, Y.-R.; Huang, R.-B.; Zheng, L.-S. *Inorg. Chem.* **2004**, *43*, 3798.

(11) (a) Luo, F.; Che, Y.-x.; Zheng, J.-m. *Cryst. Growth Des.* **2009**, *9*, 1066. (b) Reger, D. L.; Watson, R. P.; Smith, M. D. *Inorg. Chem.* **2006**, *45*, 10077. (c) Cui, Y.; Evans, O. R.; Ngo, H. L.; White, P. S.; Lin, W. B. *Angew. Chem., Int. Ed.* **2002**, *41*, 1159.

(12) (a) Zhang, K.-L.; Chang, Y.; Hou, C.-T.; Diao, G.-W.; Wu, R.; Ng, S. W. *CrystEngComm* **2010**, *12*, 1194. (b) Sarma, R.; Kalita, D.; Baruah, J. B. *Dalton Trans.* **2009**, 7428. (c) Liu, G.-X.; Huang, Y.-Q.; Chu, Q.; Okamura, T.-a.; Sun, W.-Y.; Liang, H.; Ueyama, N. *Cryst. Growth Des.* **2008**, *8*, 3233. (d) Wu, S.-T.; Long, L.-S.; Huang, R.-B.; Zheng, L.-S. *Cryst. Growth Des.* **2007**, *7*, 1746. (e) Dybtsev, D. N.; Chun, H.; Kim, K. *Chem. Commun.* **2004**, 1594. (f) Pan, L.; Liu, H.; Lei, X.; Huang, X.; Olson, D. H.; Turro, N. J.; Li, J. *Angew. Chem., Int. Ed.* **2003**, *42*, 542.

(13) (a) Yu, F.; Kong, X.-J.; Zheng, Y.-Y.; Ren, Y.-P.; Long, L.-S.; Huang, R.-B.; Zheng, L.-S. *Dalton Trans.* **2009**, 9503. (b) Wang, B.; Côté, A. P.; Furukawa, H.; O'Keeffe, M.; Yaghi, O. M. *Nature* **2008**, *453*, 207. (c) Luo, F.; Batten, S. R.; Che, Y.; Zheng, J.-M. *Chem.—Eur. J.* **2007**, *13*, 4948.

(14) (a) Zheng, B.; Dong, H.; Bai, J.; Li, Y.; Li, S.; Scheer, M. *J. Am. Chem. Soc.* **2008**, *130*, 7778. (b) Dong, Y.-B.; Jiang, Y.-Y.; Li, J.; Ma, J.-P.; Liu, F.-L.; Tang, B.; Huang, R.-Q.; Batten, S. R. *J. Am. Chem. Soc.* **2007**, *129*, 4520. (c) Fang, R.-Q.; Zhang, X.-M. *Inorg. Chem.* **2006**, *45*, 4801. (d) Forster, P. M.; Stock, N.; Cheetham, A. K. *Angew. Chem., Int. Ed.* **2005**, *44*, 7608. (e) Tong, M.-L.; Kitagawa, S.; Chang, H.-C.; Ohba, M. *Chem. Commun.* **2004**, 418. (f) Forster, P. M.; Burbanki, A. R.; Livage, C.; Férey, G.; Cheetham, A. K. *Chem. Commun.* **2004**, 368.

(15) (a) Yang, G.-P.; Wang, Y.-Y.; Liu, P.; Fu, A.-Y.; Zhang, Y.-N.; Jin, J.-C.; Shi, Q.-Z. *Cryst. Growth Des.* **2010**, *10*, 1443. (b) Wang, H.; Wang, Y.-Y.; Yang, G.-P.; Wang, C.-J.; Wen, G.-L.; Shi, Q.-Z.; Batten, S. R. *CrystEngComm* **2008**, *10*, 1583. (c) Ghosh, S. K.; Bureekaew, S.; Kitagawa, S. *Angew. Chem., Int. Ed.* **2008**, *47*, 3403. (d) Sun, R.; Wang, S.; Xing, H.; Bai, J.; Li, Y.; Pan, Y.; You, X. *Inorg. Chem.* **2007**, *46*, 8451. (e) de Lill, D. T.; Cahill, C. L. *Chem. Commun.* **2006**, 4946.

(16) (a) Wang, X. S.; Ma, S.; Forster, P. M.; Yuan, D.; Eckert, J.; Lopez, J. J.; Murphy, B. J.; Praise, J. B.; Zhou, H.-C. *Angew. Chem., Int. Ed.* **2008**, *47*, 7263. (b) Maspoch, D.; Ruiz-Molina, D.; Vaciana, J. *Chem. Soc. Rev.* **2007**, *36*, 770. (c) Cheetham, A. K.; Rao, C. N. R.; Feller, R. K. *Chem. Commun.* **2006**, 4780. (d) Mosaoka, S.; Tanaka, D.; Nakanishi, Y.; Kitagawa, S. *Angew. Chem., Int. Ed.* **2004**, *43*, 2530.

(17) (a) Gabriel, C.; Raptopoulou, C. P.; Psycharis, V.; Terzis, A.; Zevou, M.; Mateescu, C.; Salifoglou, A. *Cryst. Growth Des.* **2011**, *11*, 382. (b) Liu, T.-F.; Lü, J.; Tian, C.; Cao, M.; Lin, Z.; Cao, R. *Inorg. Chem.* **2011**, *50*, 2264. (c) Davidovicha, R. L.; Stavilab, V.; Whitmire, K. H. *Coord. Chem. Rev.* **2010**, *254*, 2193. (d) Li, D.-S.; Wu, Y.-P.; Zhang, P.; Du, M.; Zhao, J.; Li, C.-P.; Wang, Y.-Y. *Cryst. Growth Des.* **2010**, *10*, 2037. (e) Li, X.; Weng, X.; Tang, R.; Lin, Y.; Ke, Z.; Zhou, W.; Cao, R. *Cryst. Growth Des.* **2010**, *10*, 3228. (e) Liu, T.; Lv, J.; Shi, L.; Guo, Z.; Cao, R. *CrystEngComm* **2009**, *11*, 583. (f) Zhang, L.; Li, Z.-J.; Lin, Q.-P.; Qin, Y.-Y.; Zhang, J.; Yin, P.-X.; Cheng, J.-K.; Yao, Y.-G. *Inorg. Chem.* **2009**, *48*, 6517. (g) Davidovicha, R. L.; Stavilab, V.; Marinina, D. V.; Voita, E. I.; Whitmire, K. H. *Coord. Chem. Rev.* **2009**, *253*, 1316. (h) Yang, J.; Ma, J.-F.; Liu, Y.-Y.; Ma, J.-C.; Batten, S. R. *Inorg. Chem.* **2007**, *46*, 6542.

(18) Zhang, L.-P.; Lu, W.-J.; Mak, T. C. W. *Chem. Commun.* **2003**, 2830.

(19) Sheldrick, G. M. *SHELXS-97 and SHELXL-97: Program for X-ray Crystal Structure Solution*; University of Göettingen: Göettingen, Germany, 1997.

(20) (a) Zhu, H.-B.; Gou, S.-H. *Coord. Chem. Rev.* **2011**, *255*, 318. (b) Zhao, H.; Qu, Z.-R.; Ye, H.-Y.; Xiong, R.-G. *Chem. Soc. Rev.* **2008**, *37*, 84. (c) Chen, X.-D.; Wu, H.-F.; Du, M. *Chem. Commun.* **2008**, 1296. (d) Chen, X.-M.; Tong, M.-L. *Acc. Chem. Res.* **2007**, *40*, 162.

(21) (a) Li, Z.-G.; Wang, G.-H.; Jia, H.-Q.; Hu, N.-H.; Xu, J.-W. *CrystEngComm* **2007**, *9*, 882. (b) Prior, T. J.; Rosseinsky, M. J. *Inorg. Chem.* **2003**, *42*, 1564. (c) Li, J.; Yu, J.; Yan, W.; Xu, Y.; Xu, W.; Qiu, S.; Xu, R. *Chem. Mater.* **1999**, *11*, 2600. (d) Gavezzotti, A. *Acc. Chem. Res.* **1994**, *27*, 309.

(22) Li, L.-L.; Yuan, R.-X.; Liu, L.-L.; Ren, Z.-G.; Zheng, A.-X.; Cheng, H.-J.; Li, H.-X.; Lang, J.-P. *Cryst. Growth Des.* **2010**, *10*, 1929.

(23) (a) Ji, B.-M.; Deng, D.-S.; Lan, H.-H.; Du, C.-X.; Pan, S.-L.; Liu, B. *Cryst. Growth Des.* **2010**, *10*, 2851. (b) Liu, L.-L.; Ren, Z.-G.; Zhu, L.-W.; Wang, H.-F.; Yan, W.-Y.; Lang, J.-P. *Cryst. Growth Des.* **2011**, *11*, 3479.

(24) Liu, D.; Ren, Z.-G.; Li, H.-X.; Chen, Y.; Wang, J.; Zhang, Y.; Lang, J.-P. *CrystEngComm* **2010**, *12*, 1912.

(25) Du, M.; Cai, H.; Zhao, X.-J. *Inorg. Chim. Acta* **2006**, *359*, 673.

(26) Wells, A. F. *Three-Dimensional Nets and Polyhedra*; Wiley-Interscience: New York, 1977.
(27) Xu, H.; Chao, Z.; Sang, Y.; Hou, H.; Fan, Y. *Inorg. Chem. Commun.* **2008**, *11*, 1436.
(28) Pellissier, A.; Bretonnière, Y.; Chatterton, N.; Pécaut, J.; Delangle, P.; Mazzanti, M. *Inorg. Chem.* **2007**, *46*, 3714.
(29) Wei, Y.; Hou, H.; Li, L.; Fan, Y.; Zhu, Y. *Cryst. Growth Des.* **2005**, *5*, 1405.
(30) (a) Peedikakkal, A. M. P.; Vittal, J. J. *Cryst. Growth Des.* **2011**, *11*, 4697. (b) Martinez Casado, F. J.; Ramos Riesco, M.; da Silva, I.; Redondo Yelamos, M. I.; Labrador, A.; Rodriguez Cheda, J. A. *Cryst. Growth Des.* **2011**, *11*, 759.
(31) Wang, X.-L.; Chen, Y.-Q.; Gao, Q.; Lin, H.-Y.; Liu, G.-C.; Zhang, J.-X.; Tian, A.-X. *Cryst. Growth Des.* **2010**, *10*, 2174.
(32) (a) Martinez Casado, F. J.; Canadillas-Delgado, L.; Cucinotta, F.; Guerrero-Martinez, A.; Ramos Riesco, M.; Marchese, L.; Cheda., J. A. R. *CrystEngComm* **2012**, *14*, 2660. (b) Chen, S.-C.; Zhang, Z.-H.; Zhou, Y.-S.; Zhou, W.-Y.; Li, Y.-Z.; He, M.-Y.; Chen, Q.; Du, M. *Cryst. Growth Des.* **2011**, *11*, 4190. (c) Liu, X.; Guo, G.-C.; Wu, A.-Q.; Cai, L.-Z.; Huang, J.-S. *Inorg. Chem.* **2005**, *44*, 4282.
(33) Varma, R. P.; Jain, P. K. *Transition Met. Chem.* **1982**, *7*, 129.